J Mater Sci (2006) 41:5731–5734
DOI 10.1007/s10853-006-0100-1

LETTER

Modeling the effect of particle clustering on the mechanical behavior of SiC particle reinforced Al matrix composites

X. Deng · N. Chawla

Received: 14 March 2005 / Accepted: 3 October 2005 / Published online: 27 May 2006

The degree of clustering of particles has a significant influence on the mechanical behavior of particle reinforced metal matrix composites (MMCs). The clustered particles act as crack initiation sites and generally have a negative effect on tensile strength, ductility, toughness, and fatigue strength of the composite [1–10]. Murphy et al. [9] examined the tensile behavior of a 20% SiC particle reinforced Al–Si composite with different degrees of clustering (by controlling the cooling rate during solidification of the composite). It was shown that an increase in particle clustering yielded a higher work hardening rate, with a significant reduction in ductility. It has been suggested that the matrix flow in the particle cluster is significantly constrained, which results in the premature local onset of crack initiation [10–12].

Very few studies have explicitly modeled the effect of particle clustering [10–14]. Segurado et al. [10] recently investigated the effect of particle clustering on stress–strain behavior using the finite element method (FEM). They found that if particle cracking is not considered in the model, the influence of particle clustering on the predicted stress–strain behavior is not significant. While crack propagation was not explicitly modeled, the fraction of fractured particles as a function of applied strain was estimated by incorporating a Weibull distribution in strength of the particles. It was found that the presence of clustering greatly increased the fraction of fractured particles. In this study, we have conducted a two-dimensional FEM simulation to quantify the effect of clustering on local and macroscopic stress–strain behavior of Al–SiC_p composites. The models explicitly incorporate cracking of the particles for two levels of particle clustering.

Two model Al/SiC_p microstructures, consisting of circular SiC particles arranged to obtain very different degrees of clustering, were generated using image analysis (Image J, Bethesda, MD, USA). A detailed description of the image segmentation process is given elsewhere [15]. The SiC particles were represented as circular particles and the area fraction of particles was kept constant at 30%. Several techniques have been used to quantify clustering of particles in a composite [2, 16, 17]. Yang et al. [16] have shown that the coefficient-of-variance of the mean near-neighbor distance (COV_d) is particularly sensitive and effective in characterizing clustering. This parameter is also relatively insensitive to particle volume fraction, size, and morphology. COV_d can be described by the following equation [16]:

$$COV_d = \frac{\sigma_d}{d} \tag{1}$$

where σ_d is the variance in the mean nearest-neighbor distance, and d is the average of the mean near-neighbor distance.

In order to determine COV_d, a finite-body tessellation of the microstructure was created. This method is an enhancement over point-based tessellations originally derived by Dirichlet [17], where the particles occupy the center of tessellated cells, and each cell wall is equidistant between two adjacent particles. The near-neighbor distance was defined as the shortest edge-to-edge distance between two particles that share a cell wall in the tessellated image. Finally, the COV_d was calculated as the standard deviation

X. Deng · N. Chawla (✉)
Department of Chemical and Materials Engineering, Fulton School of Engineering, Arizona State University, Tempe, AZ 85287, USA
e-mail: nchawla@asu.edu

of the mean near-neighbor distances divided by the average of the mean near-neighbor distances, per Eq. 1. The microstructure with regularly distributed SiC particles had a relatively low COV_d (0.09), Fig. 1(a). The highly clustered microstructure, on the other hand, had a much higher COV_d (0.70), Fig. 1(b). Figure 1(c) shows a model microstructure and the resulting tessellated microstructure. The two microstructures were used for FEM simulations.

Finite element analysis was conducted using a commercially available software package (Abaqus 6.4, HKS, Inc., Pawtucket, RI, USA). Figure 2 shows the boundary conditions and mesh for a typical microstructure under tensile loading. The analysis was conducted in plane strain. The left edge of the model was fixed in the x-direction while the load along the x-axis was applied to the right edge of the model. Modified quadratic triangle elements were used for both the metal matrix and SiC particles. The mesh size was iteratively refined to minimize stress singularities and to achieve convergence. Mesh refinement was conducted until the overall stress–strain curve output from the model was unchanged. The elastic properties of aluminum, from experimental results, were $E = 74$ GPa, $\nu = 0.31$ [18]. The elastic properties of SiC were $E = 410$ GPa, $\nu = 0.17$ [19]. The plastic portion of the stress–strain curve for the Al matrix was taken directly from the experimental tensile stress–strain curve of 2080 Al [18]. We assumed a perfect interface between the SiC particles and Al matrix with no possibility of cracking at the Al/SiC interface. This assumption is supported by fact that the interface in powder metallurgy processed Al/SiC has a high degree of mechanical strength, and limited interfacial reaction because processing is conducted in the solid state [8]. Furthermore, fracture studies after tensile loading indicate that most of the fractured particles do not fail at the interface [20]. Cracking of the SiC particles was modeled as follows. The center plane of the particle, normal to the tensile direction was defined as an interface for crack formation and propagation. A maximum normal tensile strength was prescribed for this interface, above which decoupling of nodes (i.e., fracture) would take place. This maximum normal stress can be considered the particle strength, σ_p. In this study, for the sake of simplicity and to elucidate the effect of particle clustering only, σ_p was taken as both 1 and 2 GPa, which is in the range of strength reported for SiC particles [10, 21–23].

Figure 3 shows the simulated tensile behavior of Al–SiC composites with different degrees of particle clustering and particle strength. For a particle strength, σ_p, equal to 2 GPa, particle cracking did not take place, for the strains applied in the simulation, for both microstructures. Indeed, the stress–strain behavior for the two materials was nearly identical. This finding is consistent with the results from Segurado et al. [10]. When the particle strength was decreased to 1 GPa, particle fracture took place in both microstructures. The stochastic fracture process is represented by an abrupt drop in the stress–strain curve. Prior to crack formation, the stress–strain curve overlaps that of the simulation with $\sigma_p = 2$ GPa. After the first abrupt drop, the stress–strain curve continuously decreased, reducing the ductility of the composite significantly. The

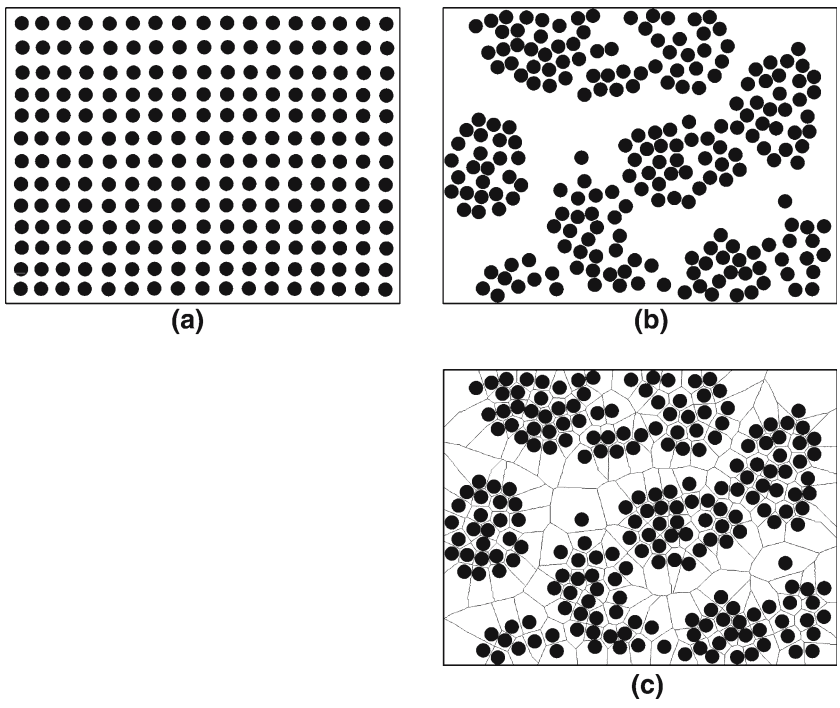

Fig. 1 Model microstructures of 30% SiC particle reinforced Al matrix composite with different degrees of particle clustering measured by COV: (**a**) $COV_d = 0.09$ and (b) $COV_d = 0.70$. Part (**c**) shows the tessellated microstructure of (**b**)

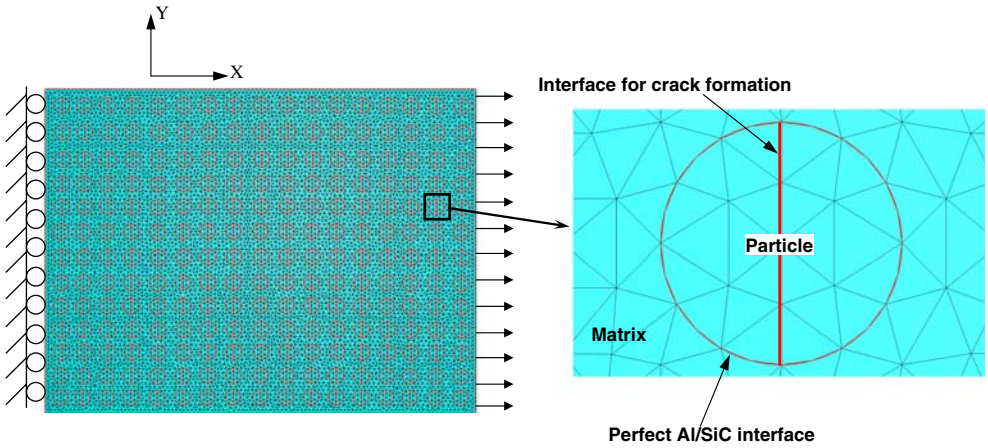

Fig. 2 Finite element mesh and boundary conditions for tensile loading simulation of the composite. Particle fracture is modeled by defining a plane along the middle of the particle, which decouples at a critical normal stress (defined here as the particle strength)

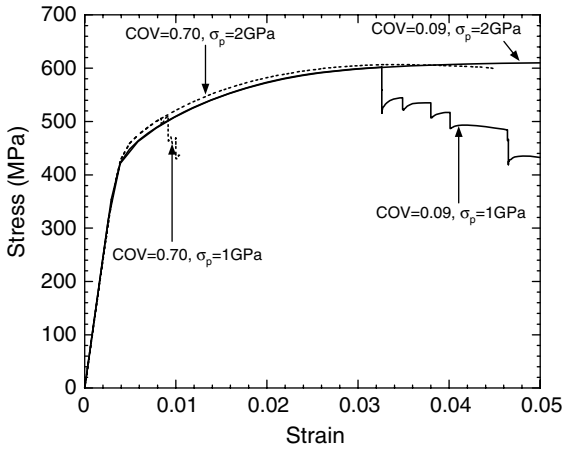

Fig. 3 Simulated tensile stress–strain curves for Al/SiC_p composites with different degrees of particle clustering and particle strength

strength and ductility of the clustered microstructure was significantly lower than that of the more homogeneous microstructure. It should be noted that the term ''ductility'' in the simulations does not represent complete fracture of the matrix, since this is not considered in these models. Nevertheless, experimental results indicate that after particle fracture, strain localization in the matrix takes place very quickly, and very little additional strain is required to completely fracture the composite [20].

Figure 4 shows the distribution of equivalent plastic strain (PEEQ) of the composite during deformation. For lower particle clustering (COV_d = 0.09), the plastic deformation of the metal matrix is homogeneous until the onset of first particle fracture. The onset of particle fracture changes the plastic deformation distribution of the metal matrix significantly. The bands of intense plastic deformation are focused at the crack tip and in the region between cracks. For higher particle clustering (COV_d = 0.07), particle fracture occurs at a much lower applied strain. The particle fracture is localized in the clustered area, leading to high local plastic deformation of the metal matrix. Compared with the highly clustered

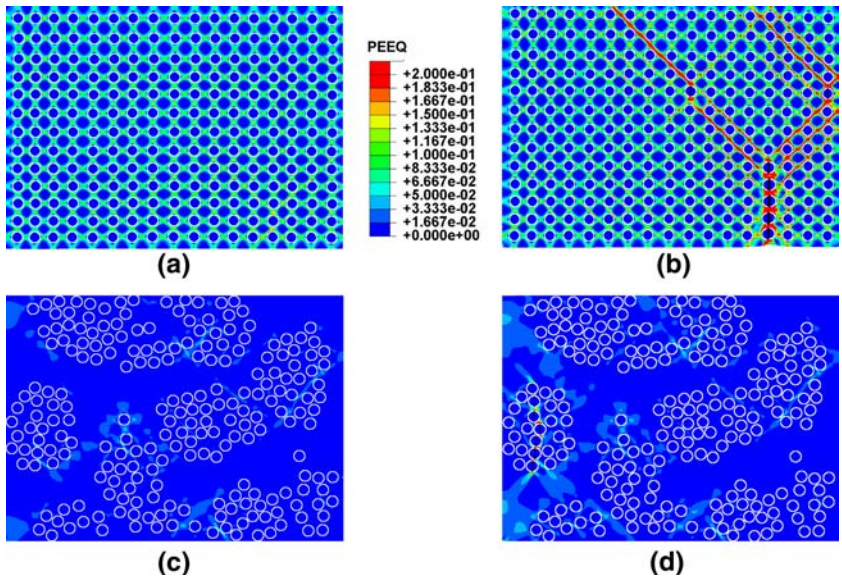

Fig. 4 Equivalent plastic strain (PEEQ) contours for: (**a**) COV = 0.09, strain of 3.3%, right before particle crack initiation, (**b**) COV = 0.09, strain of 4.0%, after particle fracture, (**c**) COV = 0.70, strain of 0.84%, right before crack initiation, and (**d**) COV = 0.70, strain of 1.0%, after particle fracture. Loading axis is horizontal

microstructure, the plastic deformation in the metal matrix was much more homogeneous in the composite with regular distribution of particles. The negative effect of particle clustering on the ductility of composite, shown by the simulations presented here, is consistent with the experimental results of Murphy et al. [9]. Further simulation studies will include the possibility of decohesion between metal matrix/particle interface and fracture of the metal matrix itself. Based on the simulation results, the following conclusions can be drawn:

1. Particle fracture has been explicitly incorporated in simulations of fracture of Al–SiC_p composites with different degrees of particle clustering.
2. When particle fracture is not considered, the particle clustering has little effect on the tensile behavior of composite. Higher particle clustering increases the work hardening of composite to a limited degree.
3. Particle clustering has a significant effect on the ductility of the composite if particle fracture is included in the simulation. Higher particle clustering leads to earlier fracture of particles due to strain localization within a particle cluster. This reduces the ductility of the composite considerably.

References

1. Chawla N, Chawla KK (2005, in press) Metal matrix composites, Springer
2. Lewandowski JJ, Liu C, Hunt WH (1989) Mater Sci Eng A 107:241
3. Nakagawa AH, Gungor MN (1989) In: Liaw PK, Gungor MN (eds) Fundamental relationships between microstructure and mechanical properties of metal–matrix composites, Warrendale, PA, TMS, pp 127–143
4. Osman TM, Lewandowski JJ, Hunt WH (1990) In: Masounave J, Hamel FG (eds) Fabrication of particulate reinforced metal composites, vol. 1, ASM International, Materials Park OH, p 209
5. Deng X, Piotrowski G, Chawla N, Narasimhan KS (2004) P/M Sci Tech Briefs 6:5
6. Chawla N, Williams JJ, Saha R (2002) J Light Metals 2:215
7. Chawla N, Davis LC, Andres C, Allison JE, Jones JW (2000) Metall Mater Trans 31A:951
8. Chawla N, Andres C, Jones JW, Allison JE (1998) Metall Mater Trans 29A:2843
9. Murphy AM, Howard SJ, Clyne TW (1998) Mater Sci Tech 14:959
10. Segurado J, Gonzalez C, Llorca J (2003) Acta Mater 51:2355
11. Mishnaevsky L Jr, Derrien K, Baptiste D (2004) Comp Sci Tech 64:1805
12. Thomson CIA, Worswick MJ, Pilkey AK, Lloyd DJ (2003) J Mech Phys Solids 51:127
13. Hutchinson JW, Mcmeeking RM (1993) In: Suresh S, Mortensen A, Needleman A (eds) Fundamentals of metal matrix composites, Butterworth–Heinemann, Boston, p 164
14. Wilkinson DS, Maire E, Embury JD (1997) Mater Sci Eng A233:145
15. http://rsb.info.nih.gov/ij/
16. Yang N, Boselli J, Sinclair I (2001) J Micros 201:189
17. Dirichlet GL (1850) J Reine Angew Math 40:209
18. Chawla N, Ganesh VV, Wunsch B (2004) Scripta Materialia 51:161
19. Chawla N, Patel BV, Koopman M, Chawla KK, Saha R, Patterson BR, Fuller ER, Langer SA (2003) Mater Charac 49:395
20. Williams JJ, Piotrowski G, Saha R, Chawla N (2002) Metall Mater Trans 33A:3861
21. Brechet Y, Embury JD, Tao S, Luo L (1991) Acta Metall Mater 39:1781
22. Llorca J, Martin A, Ruiz J, Elices M (1993) Metall Trans A 24:1575
23. Lewis CA, Whiters PJ (1995) Acta Metall Mater 43:3685